

Identification of Ionic Solutions Using a SAW Liquid Sensor

RUYEN RO, SHI-YUAN CHANG, REY-CHUE HWANG, AND DALE HUIPIN LEE

*Department of Electrical Engineering
I-Shou University
Kaohsiung, Taiwan, R.O.C.*

(Received March 5, 1999; Accepted May 19, 1999)

ABSTRACT

A method for identifying ionic solutions using a surface acoustic wave (SAW) liquid sensor is proposed in this paper. The key components of the measurement setup are a vector network analyzer, a SAW device, and an artificial intelligent identifier. The SAW device, which is fabricated on a 128° -rotated Y -cut X -propagating LiNbO_3 piezoelectric substrate, is connected to the analyzer for scattering parameter measurement. The measured transmission coefficients of ionic solutions are adopted here to calculate the phase velocity and insertion loss of SAWs over a frequency range of 32 to 35 MHz. The principal components of the measured phase velocity and insertion loss are then used to represent the corresponding solution for pattern recognition by implementing the developed identifier, which is constructed using a three-layer feed-forward neural network. Results demonstrate that a SAW device implemented with principal component analysis and a neural network can be applied effectively to identify ionic solutions.

Key Words: SAW liquid sensor, phase velocity, insertion loss, principal component analysis, neural network, pattern recognition, ionic solution

I. Introduction

Due to the recent remarkable progress in micromachining and material synthesis, surface acoustic wave (SAW) devices have been widely adopted for signal-processing and sensing applications in the microwave frequency range (Campbell, 1989; Ballantine *et al.*, 1997). SAW devices, in general, consist of input and output interdigital transducers (IDTs), which are photolithographed on piezoelectric substrates (Auld, 1973; Kino, 1987). The propagation characteristics, e.g., the phase velocity, attenuation constant and electromechanical coupling coefficient, of SAWs are functions of the material properties of the substrates and acoustoelectric properties of surface loadings (Matthews, 1977; Ro and Lee, 1997). The values of the propagation characteristics can be computed numerically by solving the Christoffel equations along with appropriate boundary conditions (Ro and Lee, 1997; Shana, 1991). The operating frequency of the SAW device can then be determined from the IDT periodicity and the SAW phase velocity.

Following the successful application of thickness shear mode (TSM) devices in gas and liquid sensors, SAW devices have been explored for their use in sensing applications due to the fact that SAW devices can be

operated at higher frequency than can TSM devices (Ballantine *et al.*, 1997; Koike *et al.*, 1993). Measurements of H_2S and SO_2 indicate that SAW gas sensors are more sensitive than TSM gas sensors (Bryant *et al.*, 1981, 1983). To further increase the measurement sensitivity of SAW gas or liquid sensors, layered structure SAW devices have been proposed and studied (Koike *et al.*, 1993; Higaki *et al.*, 1997). Results show that the SAW phase velocity of the layer structure can be increased significantly and, hence, the measurement sensitivity enhanced. In addition to the utilization of the Rayleigh SAW, different propagation modes, which can be generated by IDTs, have been investigated for their use in liquid sensing applications (Plesskii and Ten, 1986; Martin and Ricco, 1987; Jin and Joshi, 1996). Acoustic plate mode and flexural plate-wave devices have been developed for detecting the conducting and/or viscosity of liquid loadings. In lieu of one single TSM or SAW device used in designing gas or liquid sensors, array typed acoustic wave sensors have been implemented for pattern recognition. Shear horizontal SAW devices along with the principal component analysis method have been used for fruit juice and liquid identification (Kondoh and Shiokawa, 1994; Kondoh *et al.*, 1996). The neural network technique has been applied to a 12-element metal oxide sensor

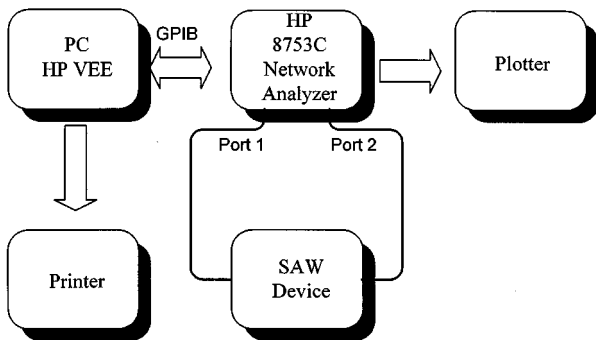


Fig. 1. Schematic diagram of the measurement system.

for odor discrimination and recognition (Gardner *et al.*, 1990).

Simulation and experimental results have revealed a relaxation phenomenon of ionic solutions in fractional velocity change and insertion loss change curves (Ro and Lee, 1997; Shana, 1991; Ro *et al.*, 1999). This relaxation phenomenon occurs when the operating frequency (angular) of the SAW device approximately equals the ratio of the conductivity to the permittivity of the liquid loading. Accordingly, a measurement system was developed for characterizing the scattering parameters (S-parameters) of a SAW device over the operating bandwidth of the device (Ro *et al.*, 1999). The measured S-parameters can then be used to study the frequency responses, e.g., phase velocity and insertion loss, of ionic solutions. As an extension of previous studies, the application of the neural network technique with/without the principal component analysis method to the analysis of measured S-parameters is investigated in this paper. Our results indicate that a Rayleigh SAW device employed using the appropriate pattern recognition technique can be used to characterize ionic solutions.

II. Experiment

The major components of the measurement system used for S-parameter measurement are a HP 8753C vector network analyzer, a personal computer, and the HP VEE data acquisition software (Ro *et al.*, 1999). A schematic diagram of the measurement system is shown in Fig. 1. The frequency range of the analyzer is from 300 KHz to 6 GHz. The full two-port calibration technique is used to minimize the effect of systematic measurement errors (Ro, 1991). The time domain gating technique is also applied to remove residual postcalibration errors as well as to get rid of unwanted bulk waves and the triple SAW (Bray *et al.*, 1987).

The geometrical size of the 128°-rotated Y-cut X-

propagating LiNbO₃ (128YX.LN) piezoelectric substrate used for the SAW device is 18×20×0.5 mm. Both input and output IDTs have five paired electrodes, which were photolithographed on 128YX.LN with 1500 Å thick aluminum. The electrode periodicity for each IDT is 29.04 μm; hence, the center frequency of the SAW device is around 34.4 MHz. The center-to-center distance between the input and output IDTs is 8.552 mm, of which around 6 mm width is reserved for liquid loadings. After a full two-port calibration technique was performed, the SAW device was connected to the measurement system for S-parameter measurement. Due to the impedance mismatch between the SAW device and the measurement system (50 Ω), the incident power was almost totally reflected. To get maximum power transfer to the SAW device, the matching networks were designed based on the measured S-parameters using the two-port impedance matching method (Bowick, 1982). The matched SAW device, as shown in Fig. 2, was used in this study to measure the propagation characteristics of SAWs. The measurement errors of the SAW phase velocities for the free and metal surfaces at 34.4 MHz were 1.2% and 0.13%, respectively, as compared with the theoretical data (Ro *et al.*, 1999). The measurement errors maybe due to transduction effects on the IDTs (Janin *et al.*, 1996).

A liquid cell with a length of 13.8 mm, an outside width of 4.4 mm, an inside width of 3.13 mm, and a height of 10 mm was designed to contain liquid loadings for S-parameter measurement. The liquid cell was placed between input and output IDTs and was attached

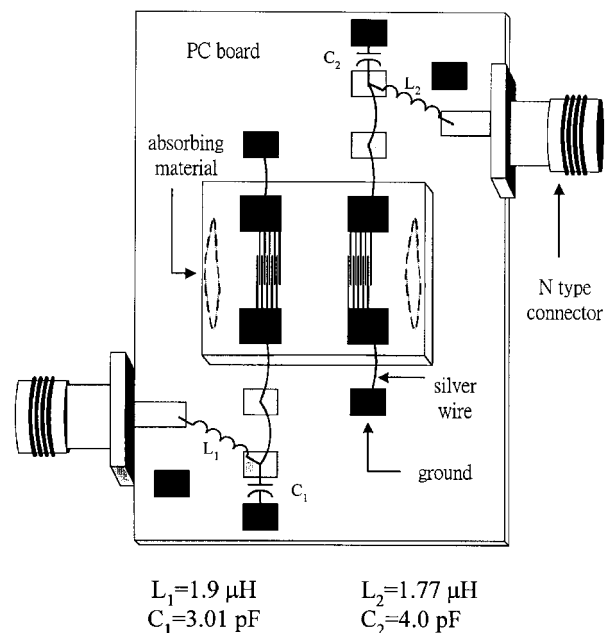


Fig. 2. Geometric configuration of the matched SAW device.

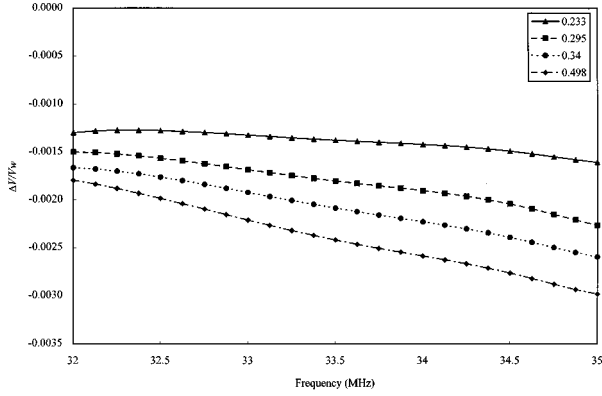


Fig. 3. Fractional velocity change versus frequency for ionic solutions with $\sigma=0.233, 0.295, 0.340,$ and 0.498 S/m.

to the substrate using polyvinyl acetate glue. The liquid loadings prepared for this study included deionized water and ionic solutions with different mass concentrations of potassium chloride (KCl). The mass concentrations of 18 KCl samples ranged from 0.02% to 1.3%, and the corresponding conductivity σ of the ionic solutions varied from 0.0355 to 2.04 S/m. After the measurement system was calibrated, the ionic solution was loaded into the liquid cell for S-parameter measurement.

III. Results and Discussion

The magnitude and phase of the measured transmission coefficients, M_{21} and θ_{21} , were adopted to calculate the SAW phase velocity and insertion loss of liquid loadings. Since the phase in the measurement system ranged from -180° to 180° , the actual phase or phase velocity could not be computed directly from the measured phase. This resulted in ambiguities associated with the calculation of the phase velocity. With the advent of time domain measurements, the unique solution of the phase velocity could be determined by analyzing the time domain signal (Varadan *et al.*, 1994). The SAW phase velocity for the liquid loading was then calculated as

$$V_l = \frac{d}{(\theta_{21l} - \theta_{21f} + 2n\pi) / \omega + d/V_f}, \quad (1)$$

where $d = 3.13$ mm is the inside width of the liquid cell, θ_{21l} and θ_{21f} are the phases of the transmission coefficient for the liquid loading and free surface, respectively, ω is the angular frequency, $V_f = 3994$ m/s is the SAW phase velocity for the free surface, and n is an integer which can be determined by analyzing the time domain signal.

The measured phase velocity and insertion loss

for four liquid loadings plotted against the frequency are shown in Figs. 3 and 4. There are 25 measured values for each curve in the frequency range of 32 to 35 MHz. The fractional velocity change $\Delta V/V_w$ shown in Fig. 3 is defined as

$$\frac{\Delta V}{V_w} = \frac{V_s - V_w}{V_w}, \quad (2)$$

where V_w and V_s are the SAW phase velocities for deionized water and ionic solution, respectively. The insertion loss change ΔM_{21} shown in Fig. 4 was calculated as

$$\Delta M_{21} = M_{21w} - M_{21s}, \quad (3)$$

where M_{21w} and M_{21s} are the magnitudes of transmission coefficients for deionized water and ionic solution, respectively. The measured 25 paired data, $\Delta V/V_w$ and ΔM_{21} , for each solution were used to represent the corresponding liquid loading in order to study the feasibility of using the SAW liquid sensor in pattern recognition.

To this end, an artificial intelligent identifier constructed using a three-layer feed-forward neural network was developed to identify the sampled solutions. A neural network of size $2-h-3$ was used as the basic structure of the identifier; i.e., there were 2 nodes in the input layer, h nodes in the hidden layer, and 3 nodes in the training case. The number of nodes h in the hidden layer was changeable based on each training case. The error back-propagation learning algorithm was adopted to train the network (Haykin, 1994). The neural identifier was trained using the known experimental data. Once the training session was completed, the trained network could then be utilized as an identifier.

Two approaches to dealing with the measured data

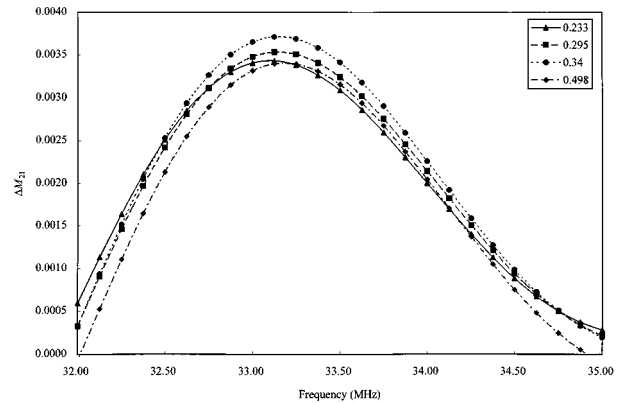


Fig. 4. Insertion loss change versus frequency for ionic solutions with $\sigma=0.233, 0.295, 0.340,$ and 0.498 S/m.

SAW Liquid Sensor Identifying Ionic Solution

were employed here before we used the identifier to recognize the liquid loadings. In the first approach, the input data for training and identifying were all of the measured 25 paired data, as shown in Figs. 3 and 4. In lieu of the measured data, their principal components were used in the second approach. The principal components of the measured data were obtained using multivariate analysis, which could be used to transform the original set of variables into a smaller set of linear combinations (Chatfield and Collins, 1980; Dillon and Goldstein, 1984). The purpose of implementing the principal component analysis was to use as few factors (principal components) as possible to sufficiently represent the variations of the measured data. The plots of the first two principal components (PC1 and PC2) of the measured data are shown in Fig. 5.

In addition to the training data, five more measurements for each ionic solution were made in this study for pattern recognition. The identification results for the sampled solutions are listed in Tables 1-3. The input data used in Tables 1, 2, and 3 are the measured 25 paired data, the first two principal components (PC1 and PC2), and the first three principal components (PC1, PC2, and PC3), respectively. The rows and columns in each table represent the sampled solutions and the identified categories, respectively. In Table 1, the recognition probabilities for the $\sigma = 0.233$ and 0.340 S/m samples are 100%; meanwhile, the $\sigma = 0.295$ and 0.498 S/m samples can not be recognized. This may have resulted from the fact that the differences among the measured data, as shown in Figs. 3 and 4, were too small to differentiate. The identification results listed in Tables 2 and 3 show that the recognition probabilities for the $\sigma = 0.233$, 0.295 and 0.498 S/m samples are 100%. For the $\sigma = 0.340$

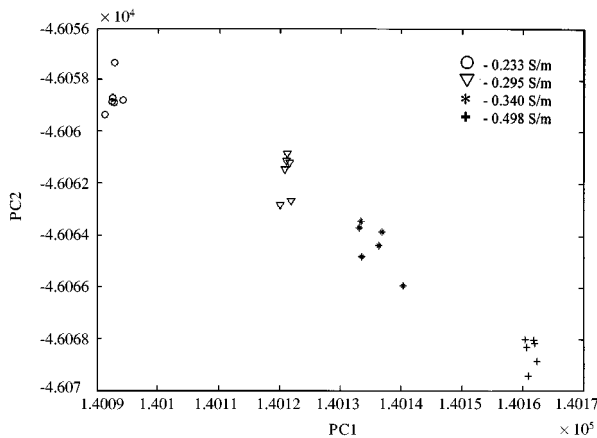


Fig. 5. Scatter diagram for ionic solutions with $\sigma=0.233$, 0.295 , 0.340 , and 0.498 S/m.

Table 1. Identification Results of Ionic Samples Using the Measured 25 Paired Data

KCl (S/m)	Identification results				
	0.233	0.295	0.340	0.498	unknown
0.233	5	0	0	0	0
0.295	0	0	5	0	0
0.340	0	0	5	0	0
0.498	0	1	0	0	4

Table 2. Identification Results of Ionic Samples Using the First Two Principal Components

KCl (S/m)	Identification results				
	0.233	0.295	0.340	0.498	unknown
0.233	5	0	0	0	0
0.295	0	5	0	0	0
0.340	0	2	3	0	0
0.498	0	0	0	5	0

Table 3. Identification Results of Ionic Samples Using the First Three Principal Components

KCl (S/m)	Identification results				
	0.233	0.295	0.340	0.498	unknown
0.233	5	0	0	0	0
0.295	0	5	0	0	0
0.340	0	1	4	0	0
0.498	0	0	0	5	0

S/m sample, the recognition probabilities listed in Tables 2 and 3 are 60% and 80%, respectively. Use of the first four or five principal components as the input data produced the same identification results as those listed in Table 3. Comparing Table 3 with Table 1, it is clear that applying principal component analysis to the measured data before identifying could increase the total recognition probability significantly. The reason behind this is that the apparent differences among the principal components of the measured data, as shown in Fig. 5. However, one and two $\sigma = 0.340$ S/m samples listed in Tables 3 and 2, respectively, still could not be recognized correctly and were identified as the $\sigma = 0.295$ S/m sample. The acoustoelectric properties of the $\sigma = 0.340$ S/m sample along with their principal components are close to those of the $\sigma = 0.295$ S/m sample over the frequency range of 32-35 MHz, as shown in Figs. 3-5. This may have caused the decrease in the recognition probability when measurement errors became significant. To increase the overall recognition probability, array-type SAW devices, which can be operated over broadband frequency ranges, will

be employed in the future to design SAW liquid sensors, and the corresponding results will be reported.

IV. Conclusions

In this paper, a measurement technique for identifying ionic solutions using a SAW liquid sensor has been presented. The SAW device, which is fabricated on a 128YX.LN piezoelectric substrate, operates in a frequency range of 32-35 MHz. An artificial intelligent identifier, constructed using a three-layer feed-forward neural network, has been developed to identify liquid samples through principal component analysis of the measured data. Identification results reveal that a Rayleigh SAW device implemented with appropriate pattern recognition software can be employed successfully as an ionic solution identifier. Based upon the results obtained, applications of these SAW liquid sensors for identification of liquid loadings differing in conductivity and/or viscosity will be studied. In addition, the feasibility of designing SAW liquid sensors using different piezoelectric substrates and/or different propagation modes as liquid identifiers will be investigated.

Acknowledgment

The authors would like to thank the National Science Council of the Republic of China for financially supporting of this research under Contracts NSC 86-2216-E-214-007 and NSC 88-2623-D-214-001.

References

- Auld, B. A. (1973) *Acoustic Fields and Waves in Solids*, Vol. 1-2. John Wiley and Sons, New York, NY, U.S.A.
- Ballantine, D. S., R. M. White, S. J. Martin, A. J. Ricco, E. T. Zellers, G. C. Frye, and H. Wohltjen (1997) *Acoustic Wave Sensors: Theory, Design, and Physico-Chemical Applications*. Academic Press, Inc., San Diego, CA, U.S.A.
- Bowick, C. (1982) *RF Circuit Design*. Howard W. Sams & Co., Inc., Indianapolis, IN, U.S.A.
- Bray, R. C., T. L. Bagwell, R. L. Jungerman, and S. S. Elliott (1987) Time-domain characterization of SAW device. In: *RF & Microwave Measurement Symposium and Exhibition*, pp. 1-19. Hewlett Packard, Santa Rosa, CA, U.S.A.
- Bryant, A., D. L. Lee, and J. F. Vetelino (1981) A surface acoustic wave gas detection. *Proc. IEEE Ultra. Symp.*, pp. 171-174. New York, NY, U.S.A.
- Bryant, A., M. Poirier, G. Riley, D. L. Lee, and J. F. Vetelino (1983) Gas detection using surface acoustic wave delay lines. *Sensors and Actuators*, **4**, 105-110.
- Campbell, C. (1989) *Surface Acoustic Wave Devices and Their Signal Processing Applications*. Academic Press, Inc., San Diego, CA, U.S.A.
- Chatfield, C. and A. J. Collins (1980) *Introduction to Multivariate Analysis*. Chapman & Hall, London, U.K.
- Dillon, C. and M. Goldstein (1984) *Multivariate Analysis: Methods and Applications*. John Wiley & Sons, New York, NY, U.S.A.
- Gardner, J. W., E. L. Hines, and M. Wilkinson (1990) Application of artificial neural networks to an electronic olfactory system. *Meas. Sci. Technol.*, **1**, 446-451.
- Haykin, S. (1994) *Neural Network: a Comprehensive Foundation*. Macmillan College Publishing Co., New York, NY, U.S.A.
- Higaki, K., H. Nakahata, H. Kitabayashi, S. Fujii, K. Tanabe, Y. Seki, and S. Shikata (1997) High power durability of diamond surface acoustic wave filter. *IEEE Trans. UFFC*, **44**, 1395-1400.
- Janin, Y., G. Feuillard, F. Teston, F. Levassort, and M. Lethieccq (1996) Simple measurement for determining surface acoustic wave velocities. *IEEE IM. Technology Conference*, pp. 247-250. Brussels, Belgium.
- Jin, Y. and S. G. Joshi (1996) Propagation of a quasi-shear horizontal acoustic wave in Z-X lithium niobate plates. *IEEE Trans. UFFC*, **43**, 491-494.
- Kino, G. S. (1987) *Acoustic Waves: Devices, Imaging, and Analog Signal Processing*. Prentice-Hall, Inc., Englewood Cliffs, NJ, U.S.A.
- Koike, J., K. Shimoe, and H. Ieki (1993) 1.5 GHz low-loss surface acoustic wave filter using ZnO/sapphire substrate. *Jpn. J. Appl. Phys.*, **32**, 2337-2340.
- Kondoh, J. and S. Shiokawa (1994) New application of shear horizontal surface acoustic wave sensors. *Jpn. J. Appl. Phys.*, **33**, 3095-3099.
- Kondoh, J., T. Imayama, Y. Matsui, and S. Shiokawa (1996) Enzyme biosensor based on surface acoustic wave device. *Electronics and Communications in Japan*, **79**, 69-73.
- Martin, S. J. and A. J. Ricco (1987) Acoustic wave viscosity sensor. *Appl. Phys. Lett.*, **50**, 1474-1476.
- Matthews, H. (1977) *Surface Wave Filters*. John Wiley and Sons, New York, NY, U.S.A.
- Plesskii, V. P. and Y. A. Ten (1986) Influence of viscous loading of the surface of an acoustic line on the propagation of shear substrate waves. *Sov. Phys. Acoust.*, **2**, 121-124.
- Ro, R. (1991) *Determination of the Electromagnetic Properties of Chiral Composites, Using Normal Incidence Measurements*. Ph.D. Dissertation. Pennsylvania State University, State College, PA, U.S.A.
- Ro, R. and M. Lee (1997) Liquid loading effects on propagation characteristics of surface acoustic waves. *J. Acoust. Soc. R.O.C.*, (in Chinese), **4**, 30-39.
- Ro, R., S. Y. Chang, and D. H. Lee (1999) Measurement of SAW liquid sensors. *Proc. Natl. Sci. Counc. ROC(A)*, **23**(2), 274-280.
- Shana, Z. A. (1991) *Theoretical Analysis of the Piezoelectric Crystal/liquid Interface for Liquid-phase-based Sensor Applications*. Ph. D. Dissertation. Marquette University, Milwaukee, WI, U.S.A.
- Varadan, V. V., R. Ro, and V. K. Varadan (1994) Measurement of the electromagnetic properties of chiral composite materials in the 8-40 GHz range. *Radio Science*, **29**, 9-22.

表面聲波液體感測器於離子溶液的辨識

羅如燕 張世源 黃瑞初 李惠嬪

義守大學電機工程學系

摘 要

在本文中，我們提出一個應用表面聲波液體感測器辨識離子溶液的方法。所使用的量測系統主要是由一個向量網路分析儀、表面聲波元件及一個人工智慧型辨識器所組成。將製作於X波傳方向128 μ m切面鋯酸鋰壓電基材的表面聲波元件連接至向量網路分析儀，可以量測出元件的散射參數。在本文中，表面聲波在32至35MHz頻率範圍內的相位速度及插入損耗是由所量測之離子溶液的傳輸係數計算而得。更進一步的，利用主成份分析法求出相位速度及插入損耗的主成份，將其代表離子溶液並利用一個由三層前饋類神經網路發展出的辨識器從事溶液辨識。結果顯示一個表面聲波元件配合主成份分析法以及類神經網路可以有效的應用於離子溶液辨識。